

# Accurate Object Association and Pose Updating for Semantic SLAM

Kaiqi Chen, Jialing Liu, Jianhua Zhang<sup>✉</sup>, Zhenhua Wang

College of Computer Science and Technology, Zhejiang University of Technology  
Hangzhou, China

**Abstract**—Nowadays in the field of semantic SLAM, how to correctly use semantic information for data association is still a problem worthy of study. The key to solving this problem is to correctly associate multiple object measurements of one object landmark, and refine the pose of object landmark. However, different objects locating closely are prone to be associated as one object landmark, and it is difficult to pick up a best pose from multiple object measurements associated with one object landmark. To tackle these problems, we propose a hierarchical object association strategy by means of multiple object tracking, through which closing objects will be correctly associated to different object landmarks, and an approach to refine the pose of object landmark from multiple object measurements. The proposed method is evaluated on a simulated sequence and several sequences in the Kitti dataset. Experimental results show a very impressive improvement with respect to the traditional SLAM and the state-of-the-art semantic SLAM method.

**Index Terms**—Visual Semantic SLAM, Object Association, Hierarchical Grouping, Multiple Object Tracking, Machine Vision

## I. INTRODUCTION

Visual Simultaneous Localization and Mapping (SLAM) currently plays an important role in Augmented Reality, Robotics, etc.. Traditional visual SLAM uses very little semantic information in localization and mapping, so that it is restricted in some application scenarios. Although the pure visual SLAM has general robust performance, it is easy to lose in dynamic scenes, fast motion, texture loss, lighting changes and other situations. Combining traditional SLAM with semantic information can improve the robustness of the system, and be more in line with human cognition of exploring unknown environments.

In the literature, researchers have proposed several semantic SLAM systems, e.g. [1]–[4]. The results show that correct object association can improve the performance of SLAM, and SLAM can also provide a better initial value for processing object association. These two aspects are tightly coupled. However, semantic information has not been fully utilized in their work. Moreover, their object association is performed in the entire environment, so all object measurements are considered at the same time, which is inefficient.

In order to improve the accuracy of data association and ensure the robustness of SLAM, we proposed a Hierarchical Dirichlet Processing (HDP)-based object association method

and implemented the corresponding semantic SLAM system in our previous work [5]. This method treats each keyframe as a group, object measurements in the same group cannot be associated with the same object landmark. For each object measurement, we only need to traverse all the keyframes that have a common view relationship with the keyframe possessing this object measurement, and determine whether to associate the same object landmark or associate to a new object landmark. Through such an association, the method achieves better accuracy for object association and higher robustness for the system.

However, this method only utilizes the position and appearance of the object measurement in world coordinates to calculate the probability when determining whether an object measurement is the same as other object measurements. Thus a flaw in this method is when object measurements have similar appearance and closing location in several adjacent keyframes, it is prone to associate object measurements that belong to different object landmarks to the same object landmark.

Furthermore, how to determine the best pose of object landmark is also a problem that has not been carefully considered by [5], where the pose of object landmark is computed from the first object measurement associated to this object landmark. However, every different object measurement associated to one object landmark has different pose in world coordinates, it is clearly unreasonable that just uses the first one as the pose of object landmark. Thus, the inaccurate pose will influence the accuracy of SLAM system.

In this study, we propose two strategies to solve these problems. First, a hierarchical keyframe grouping data association strategy is proposed, where several adjacent keyframes are formed into a keyframe group. This group is superior to a single keyframe which is treated as a group in our previous work [5]. In this keyframe group, a multiple object tracking (MOT) [6] approach is used to associate objects within the group, and to avoid wrong object associations in adjacent keyframes. And the intra-group association can further improve object associations among keyframe groups. Second, when selecting the optimal pose of the object landmark, we choose the pose of the object measurements which has the smallest distance difference and orientation deviation to other poses of object measurements associated to the same object landmark.

We carry out several experiments to verify the performance of the proposed method in a simulation sequence constructed by Airsim [7] and some real sequences in the KITTI dataset

<sup>✉</sup>Jianhua Zhang is the corresponding author, zjh@ieee.org.

[8]. Experimental results show that our method is more accurate and robustness than the original method(HDP-SLAM) [5] in terms of object association and object pose.

## II. RELATED WORK

In recent years, the combination of semantic information and SLAM has become more and more common. Semantic information combined with SLAM is mainly used in two modules: localization [9], [10] and mapping [11], [12]. By using the semantic information to assist the system localization, a relatively accurate object pose will be obtained. The key to use semantic information is object association.

Common data association methods mainly include the following, Extended Kalman Filter (EKF) [13], Expectation Maximization (EM) [1], [14] and Deep Learning methods (DL) [15], [16], etc. EKF uses the odometer to obtain the landmark information at the current moment, matches with the previous landmarks, obtains the information of the robot, and then re-estimates its own position, and finally updates the location and uncertainty of each landmark. When SLAM is initialized, the pose estimation is incorrect or the mapping is fuzzy, which can easily lead to problems in data association.

Bowman et al. [1] proposed using the EM algorithm to deal with data association problems. This method is to tightly couple inertial, geometric and semantic observations into a single optimization framework, verifying the performance of the algorithm on indoor and outdoor data sets. The EM-Fusion proposed by Strecke [14] also uses the EM algorithm for an object-level dense dynamic SLAM. This method has greatly improved the accuracy of data association and can handle object occlusion.

Xiang et al. [16] proposed to use recurrent neural network to solve the data association problem. They provide semantic tags for objects and use recursive units to connect information on multiple views. Their approach to data association is impressive. Liu et al. [15] tried to use the most advanced convolutional neural networks (CNNs) and Structure From Motion (SFM) for object detection and scene reconstruction, which can be used to identify repetitive computing scenes, and improved object data association.

In our method, we still use the advantage of the HDP method [5] that the object association is tightly coupled with SLAM. The key difference is that we have made further improvements to the original object association and pose estimation of object landmark, which greatly improved the accuracy and robustness of the SLAM system.

## III. OBJECT SLAM

In the original HDP-SLAM method [5], the object measurement information is obtained through deep learning method, i.e., the SSD model [17]. It detects objects and output 2D bounding boxes from each keyframe. Then, image patches cropped according to these bounding boxes are input into a pose prediction network [18] to obtain the 3D pose of object measurements. This processing does not take into account that the spatiotemporal correlation of object measurements in

several adjacent keyframes, where one object can be tracked in a short time with very high accuracy. Therefore this processing has two limitations. The first is that object measurements with similar appearances and closing locations observed from two adjacent keyframes may be wrongly associated. The second is that object measurements may be lost as some objects cannot be detected.

In this study, we propose to use one-step MOT [6] to detect and track object measurements in several adjacent keyframes. And we form these adjacent keyframes as a group. Thus, in this group, object association can be achieved by object tracking. Because the number of keyframes in this group is small (it is usual less than 10), object tracking is precise and object association within the group is accurate. To associate object measurements among groups, the HDP is employed as our previous HDP-SLAM [5]. After object association among groups, the pose of each object landmark will be refined by considering all poses of object measurements associated to this landmark.

### A. Object Association

In the HDP-SLAM, each keyframe is treated as a group, and the object measurement in each new keyframe is directly associated with the object landmark. It ignores the strong spatiotemporal correlation of object measurements that belong to one object landmark but are detected from several adjacent keyframes. Thus incorrect associations may occur when similar and closing objects are detected in adjacent keyframes. In order to improve the correctness of object association, we propose a hierarchical grouping strategy for object association.

As shown in Fig.1, the SLAM system selects representative frames from all frames as keyframes  $F_{1:D} = \{F_1, \dots, F_D\}$  to reduce redundant computation costs at time  $t$  in the time axis  $T$ . For adjacent  $M$  keyframes, we group them as a keyframe group. At the time  $t$ , we assume there are totally  $N$  groups. Two adjacent keyframe groups have  $j$  keyframes overlap, which adds a constraint to the object association between the keyframe groups. Thus, we denote the  $G_t = \{g_1, \dots, g_N\}$  as the keyframes we obtained at  $t$  time.

In each keyframe group, we associate object measurements through the MOT algorithm [6]. Because there is only  $M$  adjacent keyframes, where  $M$  is usual less than 10, the object measurements belonging to one object landmark can be detected and tracked with high accuracy. For object association among keyframe groups, we still utilize HDP as in [5]. But in this study, we can model multiple object measurements associated in a keyframe group, and computer the prior based on this model when executing object association among keyframe groups through Gibbs sampling in the HDP.

1) *Object Association In Keyframe Group*: In a keyframe group, we employ FairMOT [6] for object detection and tracking. For a keyframe  $F_m$ , a set of object measurements  $L_m = \{L_{m,1}, \dots, L_{m,K_d}\}$  can be obtained, where  $K_m$  means the number of object measurements that are detected and tracked. For a object measurement  $L_m^k$ , it contains all information that is required in the following object association,

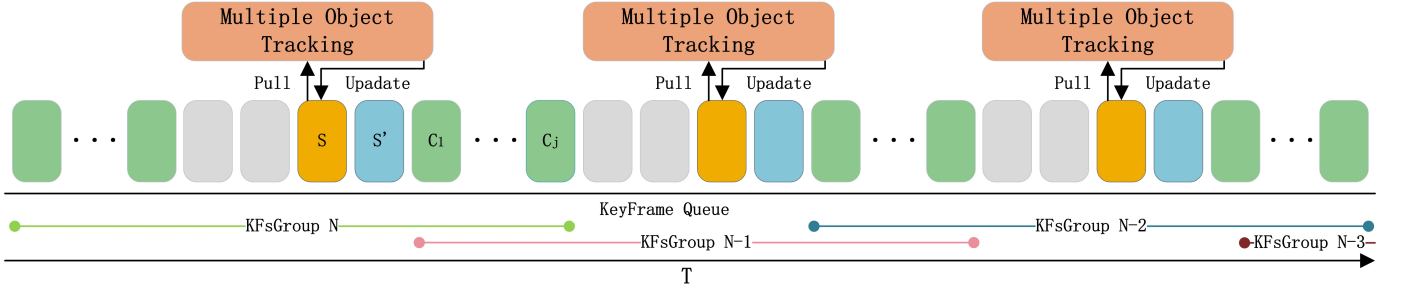


Fig. 1. KeyFrame Queue: In this timeline  $T$ , the keyframe  $S$  (yellow) is about to enter multi-target tracking. The keyframe  $S'$  (blue) has been detected and tracked, and the frame acquired objects information. The keyframe queue is divided into keyframe groups  $N$ , and adjacent keyframe groups overlap  $j$  keyframes (green).

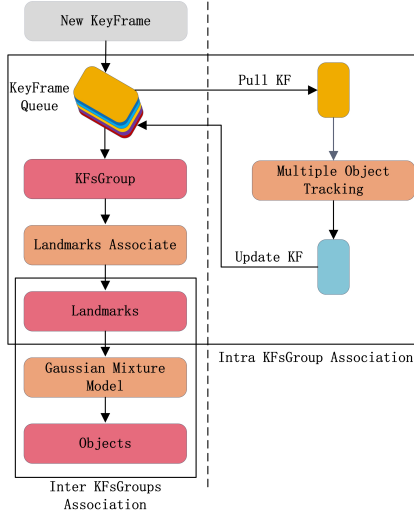


Fig. 2. Each keyframe is added to the keyframe queue and handle object association intra and inter groups of keyframes. Intra Group Association: the yellow keyframe turns into blue keyframe after multi-target detection, and the blue key frame contains object measurement information. Inter Group Association: the objects in the keyframe group are processed by GMM to obtain the final real objects.

$$L_{m,k} = \{Id_{m,k}^{obj}, Id_{m,k}^{kf}, x_{m,k}, y_{m,k}, w_{m,k}, h_{m,k}\}, \quad (1)$$

where  $Id_{m,k}^{obj}$ ,  $Id_{m,k}^{kf}$ ,  $x_{m,k}$ ,  $y_{m,k}$ ,  $w_{m,k}$ ,  $h_{m,k}$  are the detected object ID, the keyframe ID, x-axis and y-axis coordinate, width and height of the detected bounding box, respectively.

In general, one object landmark can be observed as multiple object measurements in several adjacent keyframes. Thus, in a keyframe group, several object measurements of one object landmark can be detected. Through the FairMOT, these object measurements can be efficiently and accurately associated to one object landmark, as it can simultaneously track multiple object instances across several keyframes. In the  $n$ th keyframe group, we denote the association between the  $k$ th object measurement in the  $m$ th keyframe (i.e.  $L_{m,k}^G$ ) and the  $i$ th object landmark as  $s_{n,i}^{m,k} = \langle O_{n,i}^G, L_{m,k}^G \rangle$ , where the superscript  $G$  denotes the association is within one keyframe group. If an object measurements is detected and

cannot be associated to any previous object measurements, a new object landmark is generated. Finally, we have a set of object landmarks in the level of one keyframe group, denoted as  $O_n^G = \{O_{n,1}^G, \dots, O_{n,I}^G\}$ . It should be noted that these object landmarks are not the final object landmarks used in the map, and will be associated in global level. This is because that we design a hierarchical group strategy, and consequently the same hierarchical object association.

For each object landmark  $O_{n,i}^G$  in the keyframe group, there is usual more than one object measurements associated to it. Thus, we can describe the object landmark in a more precise manner, through which the object association among keyframe groups will be more accurate and robust.

2) *Object Association Among KeyFrame Groups*: When using HDP to associate objects between groups where each group is just a keyframe, HDP-SLAM computes the prior information by the location and appearance difference between object measurement and object landmark. This method is easy to be affected by inaccurate measurement and the change of environmental and lighting conditions, resulting in some wrong correlation. In this study, the basic element of object association between keyframe groups is no longer a single object measurement detected in each keyframe, but the object landmark associated by object measurements within each keyframe group. Because the object landmarks in a keyframe group are usually associated with multiple object measurements, it can provide more pose and appearance information for the landmarks in such a group, and thus it is more robust to inaccurate measurement and condition changes.

In this study, we employ Gaussian Mixture Model (GMM) [19] to model the pose information for multiple object measurements associated to one object landmark in a keyframe group.

$$\Gamma(O | \Theta) = \sum_{z=1}^Z \lambda_z \phi(O | \Theta_z) \quad (2)$$

where  $\lambda_z$  is the weight coefficient,  $\phi(O | \Theta_z)$  is the Gaussian distribution density,  $\Theta_z = \{\mu_z, \sigma_z^2\}$ , and

$$\phi(O | \Theta_z) = \frac{1}{\sqrt{2\pi}\sigma_z} \exp\left(-\frac{(O - \mu_z)^2}{2\sigma_z^2}\right) \quad (3)$$

In Equation 2, the object landmark  $O$  is associated with the information of  $Z$  object measurements, and each observation data is set with six free variables, namely the 3D world position and the orientation of the three axes of the object.

As described in HDP-SLAM [5], the prior of object pose used for Gibbs sampling to determine which object measurements should be associated is computed as the proportion of distance between object measurements. In our method, we improve this prior probability by using the above GMM. When determining if the  $i$ th object landmark  $O_{n,i}^G$  in the  $n$ th keyframe group can be associated with the  $j$ th object landmark  $O_{m,j}^G$  in the  $m$ th keyframe group, we compute the probabilities of all object measurements associated to  $O_{n,i}^G$  with respect to the GMM constructed by  $O_{m,j}^G$ , and select the maximum probability value for the following Gibbs sampling. Because there are several overlapping keyframes between two adjacent keyframe groups, some object measurements in these keyframes may be associated to two object landmarks belonging to two different keyframe groups. Thus, when executing object association among keyframe groups, the prior probability that two object landmarks can be associated is higher than other object landmarks. We enhance the probability by a scale parameter, which is set to 1.5 in our experiments.

Finally, a object landmark  $O_{n,i}^G$  in a keyframe group is assigned a unique object landmark id  $p$  in the global map, i.e.  $q_p = \langle O_p, O_{ni}^G \rangle$ . We assume there are  $P$  object landmarks in the map at time  $t$ .

As shown in Fig.2, the small solid box describes the object association process between keyframe groups. Through the object association of GMM, the real object landmark is finally obtained.

#### B. Position And Orientation Optimization Of Object Landmark

After object association in the global map, each object landmark has associated multiple object measurements. How to determine the pose of this object landmark should be carefully considered. Because the accurate pose of object landmark can help the optimization of SLAM backend, and consequently can lead to more accurate and robust localization and mapping. In the HDP-SLAM [5], the pose of first object measurement associated to one object landmark is used as the pose of this landmark, which is obviously not reasonable.

In this study, we take all pose of object measurements associated to one object landmark into account. For each object measurement, the distance between it and other object measurements is computed, and the pose of one object measurement that has the smallest distance is used as the pose of object landmark. The average angle difference ( $\theta_k$ ) and the average distance difference ( $\varphi_k$ ) of the  $k$ th object measurement to others associated to the same object landmark is computed. Because the dimension of distance and angle is different, we need to normalize them. We set the maximal angle difference  $A$  and maximal distance difference  $B$ , then the normalized average angle difference and average distance difference are computed as:

$$\bar{\theta}_k = \begin{cases} 1 & \text{if } \theta_k > A \\ \theta_k/A & \text{otherwise} \end{cases} \quad (4)$$

$$\bar{\varphi}_k = \begin{cases} 1 & \text{if } \varphi_k > B \\ \varphi_k/B & \text{otherwise} \end{cases} \quad (5)$$

The pose difference of the  $k$ th object measurements associated to the object landmark  $O_p$  is then computed as:

$$f_{O_p}(L_k) = \alpha \times \bar{\theta}_k + \beta \times \bar{\varphi}_k \quad (6)$$

where  $\alpha$  and  $\beta$  are the weights for angle and position difference, respectively. In our all experiments, we set them to 0.4 and 0.6, respectively. Then we sort all pose difference and set the pose of object landmark to the pose of the object measurement who has the minimal pose difference.

## IV. EXPERIMENT RESULTS

To evaluate the proposed method comprehensively, we carry out two kinds of experiments. One is to verify the improvements of object association by the proposed hierarchical grouping and association strategy. Another is to verify the accuracy of the pose of object landmarks. Our experiments are executed on a simulation sequence and several real sequences in the KITTI [8] dataset. Our simulation sequence is built in the outdoor scene of Microsoft AirSim [7], which approximated the real-world environment and also used in the HDP-SLAM [5]. The real sequences used in our experiments are 03, 04, 05, 06, 07, 10 sequence of KITTI odometry datasets. In order to better evaluate the correctness of our association method, we label a large number of object tags on these sequences, so that the same object has its own ID and the ID of the corresponding frame. Our SLAM system is run on a 3.6GHz eight-core Linux system with RTX2070 graphics card.

TABLE I  
COMPARISON OF EXPERIMENTAL RESULTS OF SIMULATED DATASET.

Methods	Ours RGBD	HDP-SLAM RGBD	ORB_SLAM2 RGBD
RMSE(m)	<b>0.46538</b>	0.490655	0.520598
Real objects	21	21	—
Object measurements	457	229	—
Detection objects	453	173	—
KFsGroup objects	180	173	—
Objects	<b>21</b>	13	—
Detection accuracy(%)	<b>99.13</b>	75.21	—
Association accuracy(%)	99.78	—	—

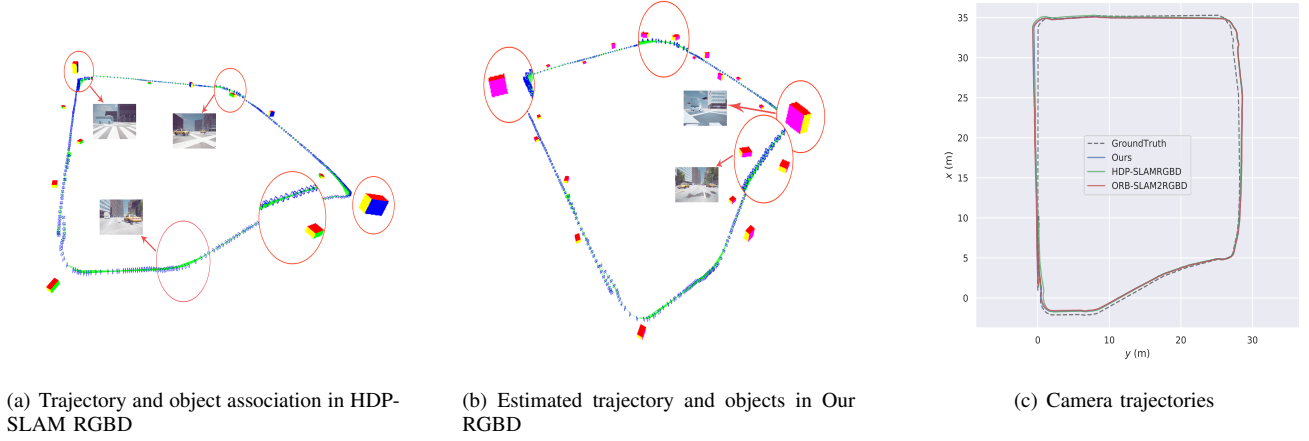


Fig. 3. The results on the simulation dataset. In the left two pictures, the big cuboid represents for the bus and the small ones are cars. The main difference between HDP-SLAM and our method is marked by red circles.

#### A. Accuracy evaluation on the Simulation Dataset

In the outdoor simulation sequence, we increase the difficulty with respect to the simulation sequence used in HDP-SLAM [5], by adding more buses and cars into the scene. We also change the position and orientation of some vehicles so that some cars or buses with the similar appearance are in very close positions. In Fig.3, we compare our method with the HDP-SLAM and original ORB-SLAM2 RGBD. It can be seen from Fig.3(a) and Fig.3(b) that all vehicles (totally 21 vehicles in this sequence) have been correctly detected and associated, and have more accurate pose by comparison with the HDP-SLAM. In Fig. 3(c), we show the camera trajectories of the three systems and the real trajectories. It is obvious that the camera trajectories of our system are closer to the Ground Truth, which is inseparable from our precise object association.

We compare the absolute trajectory error in Table I, which dropped by 10.61% and 5.15% on ORB-SLAM2 RGBD and HDP-SLAM RGBD, respectively. We use the MOT model to detect objects, and the object detection rate has increased from 75.21% to 99.13%, which provides more object measurements information for object association. At the same time, the object association in our keyframe groups provide a great help for the object association between keyframe groups, dividing 453 object measurements into 180 different object landmarks in keyframe group. The number of object landmarks after the object association among keyframe groups is 21, which is just equal to the number of real objects in the sequence. Moreover, the accuracy of our object association can reach 99.78% (mean of ten experiments).

According to these experimental results, the proposed hierarchical grouping and object association is extremely useful and necessary. Besides, to employ the MOT for object association within keyframe group can essential improve the object detection.

#### B. System performance on KITTI Dataset

In order to demonstrate the performance of our method in a real environment more comprehensively, we carry out experiments on the 03, 04, 05, 06, 07 and 10 sequences in KITTI dataset, in which we manually label all vehicles.

The object association effect of our method in these sequences is shown in Table II. On behalf of the hierarchical object association strategy, the accuracy and robustness of object association is very high. No matter that it is in 05, 06, and 07 sequences with more vehicles, or in 03, 04, and 10 sequences with fewer vehicles, our object correlation rate is more than 99%, especially in 04, 06, and 10 sequences, it achieves 100.00% correctness rate. At the same time, MOT is also a great help for the association of objects in the keyframe group. The number of objects in 03, 04, 05, 06, 07, and 10 has decreased by 54.58%, 41.18%, 49.44%, 50.71%, 59.64%, respectively.

The 04 sequence is in the highway environment, and the car is moving forward dynamically. According to the experimental data and effects, our system is very robust in traditional dynamic SLAM, and the object association is very high too. The absolute trajectory error of the camera is still smaller than other methods.

Table III shows the comparison of the absolute trajectory error of our method, HDP-SLAM Mono and ORBSLAM2 Mono in all sequences. According to the experimental results, the error of our semantic SLAM (mean value of ten experiments) is generally smaller than that of HDP-SLAM and ORBSLAM2. The error of the 07 sequence is smaller than that of ORBSLAM2, but slightly larger than that of HDP-SLAM. We guess that is because our method can detect more vehicles than HDP-SLAM, and one of them has an error in object association, which leads to a deviation in the object optimization to the camera trajectory adjustment.

In terms of the detection accuracy, our method is much higher than that of HDP-SLAM Mono. Our average detection value is 80.47%, while the average detection value

TABLE II  
OBJECT ASSOCIATION RESULTS OF OUR MONOCULAR SYSTEM IN THE KITTI DATASET.

Sequence	Object_GT	Ours Mono				
	Objects number	Object measurements	Detection objects	KFsGroup objects	Objects	Association accuracy(%)
KITTI 03	11	280	196	90	11	99.55
KITTI 04	12	59	51	30	12	100.00
KITTI 05	92	1010	797	403	91	99.83
KITTI 06	66	897	611	308	66	100.00
KITTI 07	105	1228	913	450	101	99.34
KITTI 10	15	358	332	134	15	100.00

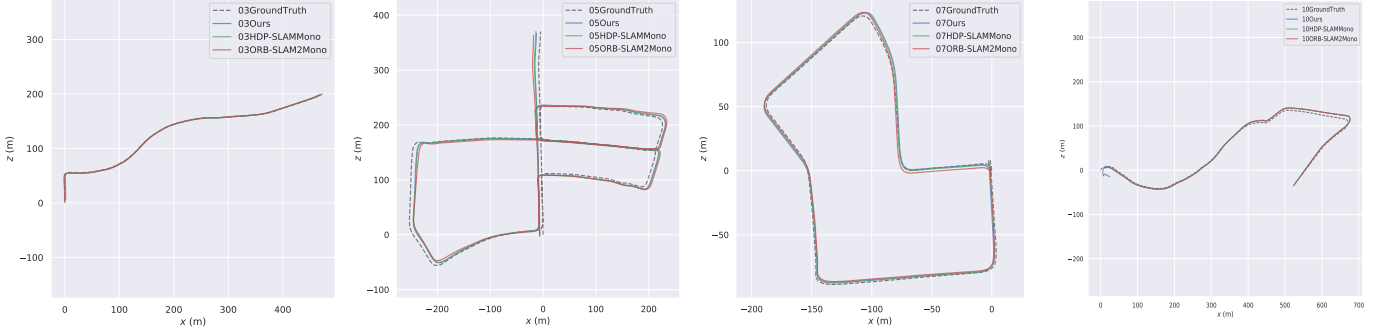


Fig. 4. The trajectory comparison results of 03, 05, 07, and 10 sequences.

TABLE III  
COMPARISON OF ABSOLUTE TRAJECTORY ERRORS OF KITTI DATASET IN DIFFERENT SYSTEMS.

Sequence	Ours Mono	HDP-SLAM Mono	ORB-SLAM2 Mono
	RMSE(m)	RMSE(m)	RMSE(m)
KITTI 03	<b>1.418593</b>	1.937704	1.475555
KITTI 04	<b>0.760534</b>	0.984562	1.188614
KITTI 05	<b>5.714461</b>	6.214913	6.746234
KITTI 06	<b>11.591997</b>	12.974504	13.532055
KITTI 07	2.395944	<b>1.877793</b>	2.445708
KITTI 10	9.375104	<b>8.957115</b>	9.407750

TABLE IV  
COMPARISON OF OBJECT MEASUREMENTS DETECTION ACCURACY.

Sequence	Ours Mono	HDP-SLAM Mono
	Detection accuracy(%)	Detection accuracy(%)
KITTI 03	<b>75.66</b>	52.94
KITTI 04	<b>85.74</b>	57.31
KITTI 05	<b>86.85</b>	62.75
KITTI 06	<b>68.12</b>	38.24
KITTI 07	<b>73.75</b>	34.09
KITTI 10	<b>92.74</b>	57.94

of HDP-SLAM can only reach 50.54%, as shown in Table IV. This is because we adopt the MOT for object detection and tracking, which takes the spatiotemporal information into account.

We further shows the camera trajectories obtained of our method, HDP-SLAM, ORB-SLAM2, and ground truth for 03, 05, 07 and 10 sequences, as shown in Fig.4<sup>1</sup>. Compared with HDP-SLAM, our semantic SLAM is more robust to static objects and dynamic objects. In our method, we select the optimal target objects, which can effectively deal with the position and orientation of dynamic objects. This provides an important idea for us to join dynamic SLAM in our future

work.

## V. CONCLUSION

In this study, we propose a hierarchical object association and keyframe grouping strategy, and the object pose refinement approach, through which the accuracy and robustness of semantic SLAM can be improved. By comparison with state-of-the-art semantic SLAM system (i.e., the HDP-SLAM), the experimental results show that our method is more efficient, and can achieve satisfactory performance.

In future work, we will further improve the accuracy of multi-target detection and increase the types of object recognition, which has shown the superiority of MOT in our method. We also plan to extend the method to the scenario of multiple agents and the applications of AR.

<sup>1</sup>The tool used to plot the result is from: [github.com/MichaelGrupp/evo](https://github.com/MichaelGrupp/evo)

## REFERENCES

- [1] S. L. Bowman, N. Atanasov, K. Daniilidis, and G. J. Pappas, "Probabilistic data association for semantic slam," in *2017 IEEE international conference on robotics and automation (ICRA)*. IEEE, 2017, pp. 1722–1729.
- [2] B. Mu, S.-Y. Liu, L. Paull, J. Leonard, and J. P. How, "Slam with objects using a nonparametric pose graph," in *2016 IEEE/RSJ International Conference on Intelligent Robots and Systems (IROS)*. IEEE, 2016, pp. 4602–4609.
- [3] R. F. Salas-Moreno, R. A. Newcombe, H. Strasdat, P. H. Kelly, and A. J. Davison, "Slam++: Simultaneous localisation and mapping at the level of objects," in *Proceedings of the IEEE conference on computer vision and pattern recognition*, 2013, pp. 1352–1359.
- [4] A. Rosinol, M. Abate, Y. Chang, and L. Carlone, "Kimera: an open-source library for real-time metric-semantic localization and mapping," in *2020 IEEE International Conference on Robotics and Automation (ICRA)*. IEEE, 2020, pp. 1689–1696.
- [5] J. Zhang, M. Gui, Q. Wang, R. Liu, J. Xu, and S. Chen, "Hierarchical topic model based object association for semantic slam," *IEEE transactions on visualization and computer graphics*, vol. 25, no. 11, pp. 3052–3062, 2019.
- [6] Y. Zhan, C. Wang, X. Wang, W. Zeng, and W. Liu, "A simple baseline for multi-object tracking," *arXiv preprint arXiv:2004.01888*, 2020.
- [7] S. Shah, D. Dey, C. Lovett, and A. Kapoor, "Airsim: High-fidelity visual and physical simulation for autonomous vehicles," in *Field and service robotics*. Springer, 2018, pp. 621–635.
- [8] A. Geiger, P. Lenz, C. Stiller, and R. Urtasun, "Vision meets robotics: The kitti dataset," *The International Journal of Robotics Research*, vol. 32, no. 11, pp. 1231–1237, 2013.
- [9] R. Mur-Artal and J. D. Tardós, "Orb-slam2: An open-source slam system for monocular, stereo, and rgb-d cameras," *IEEE Transactions on Robotics*, vol. 33, no. 5, pp. 1255–1262, 2017.
- [10] C. Campos, R. Elvira, J. J. G. Rodríguez, J. M. Montiel, and J. D. Tardós, "Orb-slam3: An accurate open-source library for visual, visual-inertial and multi-map slam," *arXiv preprint arXiv:2007.11898*, 2020.
- [11] K.-N. Lianos, J. L. Schonberger, M. Pollefeys, and T. Sattler, "Vso: Visual semantic odometry," in *Proceedings of the European conference on computer vision (ECCV)*, 2018, pp. 234–250.
- [12] J. McCormac, R. Clark, M. Bloesch, A. Davison, and S. Leutenegger, "Fusion++: Volumetric object-level slam," in *2018 international conference on 3D vision (3DV)*. IEEE, 2018, pp. 32–41.
- [13] J. Neira and J. D. Tardós, "Data association in stochastic mapping using the joint compatibility test," *IEEE Transactions on robotics and automation*, vol. 17, no. 6, pp. 890–897, 2001.
- [14] M. Strecke and J. Stuckler, "Em-fusion: Dynamic object-level slam with probabilistic data association," in *Proceedings of the IEEE International Conference on Computer Vision*, 2019, pp. 5865–5874.
- [15] X. Liu, S. W. Chen, C. Liu, S. S. Shivakumar, J. Das, C. J. Taylor, J. Underwood, and V. Kumar, "Monocular camera based fruit counting and mapping with semantic data association," *IEEE Robotics and Automation Letters*, vol. 4, no. 3, pp. 2296–2303, 2019.
- [16] Y. Xiang and D. Fox, "Da-rnn: Semantic mapping with data associated recurrent neural networks," *arXiv preprint arXiv:1703.03098*, 2017.
- [17] W. Liu, D. Anguelov, D. Erhan, C. Szegedy, S. Reed, C.-Y. Fu, and A. C. Berg, "Ssd: Single shot multibox detector," in *European conference on computer vision*. Springer, 2016, pp. 21–37.
- [18] S. Tulsiani and J. Malik, "Viewpoints and keypoints," in *Proceedings of the IEEE Conference on Computer Vision and Pattern Recognition*, 2015, pp. 1510–1519.
- [19] D. A. Reynolds, "Gaussian mixture models," *Encyclopedia of biometrics*, vol. 741, 2009.